JBUON 2020; 25(5): 2293-2300
ISSN: 1107-0625, online ISSN: 2241-6293 • www.jbuon.com
Email: editorial_office@jbuon.com

ORIGINAL ARTICLE

Anticancer effects of α-mangostin in OVACAR-3 human ovarian carcinoma cells are mediated via involvement of reactive oxygen species, mitochondrial –mediated apoptosis, suppression of cell migration and invasion and m-TOR/PI3K/AKT signaling pathway

Yi Yu, Zhiyi Fei, Li Qin

Department of Gynaecology and obstetrics, Wuhan City Puren Hospital, Wuhan, Hubei, China, 430081

Summary

Purpose: *a-mangostin belongs to xanthone class of natural products, showing a great biological and pharmacological potential. a-mangostin has shown remarkable anticancer potential against different cancer cell lines. Herein, a-mangostin was tested for its anticancer potential against human ovarian cancer cell line (OVACAR-3). Its effects on reactive oxygen species (ROS), mitochondrial-mediated apoptosis, cell migration and invasion and m-TOR/PI3K/AKT signaling pathway, was also determined.*

Methods: *MTT assay was performed to evaluate the rate of proliferation and clonogenic assay was used to assess the effects of a-mangostin on OVACAR-3 cell colonies. Phase contrast microscopy was implemented to evaluate cellular morphology. Acridine orange (AO) and ethidium bromine (EB) staining was used to check apoptosis along with western blotting. JC-1 and DCFH-DA staining assays were performed for the determination of mitochondrial membrane potential (MMP) and ROS, respectively. Cell migration and invasion analysis was performed with transwell chambers assay. The effect on m-TOR/PI3K/AKT signaling pathway was monitored by western blotting assay.*

Results: *a-mangostin had a tremendous inhibitory effect on cell proliferation rate in OVACAR-3 cells in a dose-dependent manner. The number of colonies was also observed to decline in a dose-dependent manner. Phase contrast microscopy showed significant morphological changes in OVACAR-3 cells after a-mangostin exposure. The antiproliferative effects were due to mitochondrial-mediated apoptosis. MMP was decreased by a-mangostin exposure and ROS production enhanced dose-dependently. Cell migration and invasion were also decreased by a-mangostin in OVACAR-3 cells. Finally, a-mangostin was observed to block the m-TOR/PI3K/AKT signaling pathway in OVACAR-3 cells.*

Conclusion: *a-Mangostin could induce antiproliferative effects against OVACAR-3 cells mediated via ROS production, mitochondrial-mediated apoptosis and inhibition of m-TOR/PI3K/AKT signalling. Therefore, it may prove a lead molecule in ovarian cancer treatment.*

Key words: *ovarian cancer, xanthones, a-mangostin, apoptosis, cell migration*

Introduction

Ovarian cancer is a frequent gynecologic malignancy globally [1,2]. In most of the patients, ovarian cancer is asymptomatic until advanced stages [3]. This leads to limited 5-year overall survival rates extending from 20 to 30%. Moreover, the appearance of chemotherapeutic resistance and frequent recurrences result in high mortality and very poor prognosis in ovarian cancer pa-

Corresponding author: Li Qin, MD. Department of Gynaecology and Obstetrics, Wuhan City Puren Hospital, Wuhan, Hubei, China, 430081.
Tel/Fax: +86 027 86362972, Email: 3295893973@qq.com
Received: 30/03/2020; Accepted: 21/04/2020

tients [4,5]. Consequently, to improve the survival chances in patients, refined therapeutic strategies, approaches and search for novel anticancer agents are immediately needed to successfully treat ovarian cancer. Up until today, several plant-based natural products have been isolated and used against different human diseases including cancer [6,7]. Natural products are the complementary approach for cancer treatment and act as basis of traditional Chinese medicine (TCM) [8]. Mangosteen Linn (Garcinia mangostana) is a fruit prevalent in south Asian countries like Myanmar, India and Sri Lanka. Due to exclusive and appetizing taste, the fruit is famously referred as "queen of fruits" [9]. The fruit is being used in traditional medicine since hundreds of years to manage wounds, dysentery, abdominal pain, skin infections and trauma, especially using the pericarp of the fruit [10]. In addition, mangosteen fruit is full of secondary metabolites like oxygenated and prenylated xanthones [11]. α-mangostin is present in high concentrations in the fruit and other parts of the plant as well, and has yellowish appearance. The chemical structure of α-mangostin was elucidated by Murakami (1932) and Dragendorff (1930) [12]. α-mangostin is an active xanthone holding a great biological and pharmacological potential. It has been shown to exert anti-obesity, anti-oxidant, anti-parasitic, anti-fungal, anti-bacterial, anti-diabetic, cardioprotective, anti-inflammatory as well as anti-tumor potentials. It also has been reported to achieve complete inhibition of proliferation in human leukemia HL60 via stimulation of apoptosis [13]. Furthermore, it activates apoptosis in rat pheochromocytoma PC12 cells through mitochondrial pathway by targeting Ca^{2+}-ATPase [14]. Moreover, α-mangostin has been reported to inhibit cell cycle in colon cancer cells along with induction of apoptosis [15]. This molecule inhibits the activity of MMP-2/MMP-9 in A549 lung adenocarcinoma cells via suppression of phorbol 12-myristate 13-acetate and also targets NF-κβ and αvβ3 Integrin/FAK/ERK signaling pathway [16]. Therefore, the current study was designed to investigate the anticancer effects of α-mangostin in OVACAR-3 human ovarian carcinoma cells. Involvement of reactive oxygen species (ROS), mitochondrial-mediated apoptosis, suppression of cell migration and invasion and m-TOR/PI3K/AKT signaling pathway, were also investigated.

Methods

Estimation of cellular proliferation rate

To determine the rate of proliferation in OVACAR-3 ovarian cancer cells, MTT assay was employed. 2.5×10^4 OVACAR-3 cells were placed in 96-well plates under humidified conditions in a 5% CO_2 incubator and precultured for 24h at 37°C. Preculturing was followed by α-mangostin exposure in varying time intervals (12h, 24h and 48h) and with varying doses (0, 5, 25, 50, 100 and 200 μM). Afterwards, α-mangostin-treated OVACAR-3 cells were supplemented with MTT solution (10 mg/ml) and subjected to further 4 h-incubation. MTT solution resulted in the generation of formazan crystals, which were then dissolved in DMSO (250 μL). Finally, a microplate reader (ELX 800; Bio-tek Instruments, Inc., Winooski, United States) was used to determine the absorbance at 490nm wavelength for optical density (OD) assessment.

Clonogenic potential assessment

To measure the clonogenic potential of OVACAR-3 cells, clonogenic assay was performed. 350 OVACAR-3 colonies were placed in 6-well plates and left to adhere for 12h. Afterwards, variant α-mangostin doses (0, 25, 100 and 200 μM) were added to each plate and left untouched on incubation for 48h. Then, fresh RMPI-1640 medium was inserted into each well of 6-well plates and cell colonies were thereafter cultured for 12 days. OVACAR-3 cell colonies were then collected and fixed with 4% paraformaldehyde and staining was commenced by crystal violet. Finally, stained cells were examined under a light microscope (Nikon, Japan) and colonies with >0.5mm diameter were considered for calculations.

Morphological assessment via phase contrast microscopy

Morphology of α-mangostin-treated OVACAR-3 cells was observed through phase contrast microscopy. In brief, 4×10^4 human OVACAR-3 cells were incubated with variant α-mangostin drug doses (0, 25, 100 and 200 μM) for two consecutive days within 24-well plates. After two days of incubation, RMPI-1640 medium was completely decanted and cells were washed using phosphate buffered saline (PBS). Finally, morphological alterations in treated OVACAR-3 cells against untreated controls were observed under 200x magnification of a phase contrast inverted microscope (Leica DMI 3000B, Germany).

AO/EB staining assay

Apoptosis inducing potential of α-mangostin was examined in OVACAR-3 cells by performing AO/EB staining assay. Briefly, OVACAR-3 cells were harvested with full confluence and trypsinized with trypsin (0.25%). Afterwards, a concentration of 2×10^4 trypsinized cells/ml were placed in 96-well plates with fetal calf serum (FCS). Each well plate of was supplemented with α-mangostin drug at variant concentrations (0, 25, 100 and 200 μM) followed by incubation at 37°C. Afterwards, trypsinisation was again accomplished with 20 μl of trypsin, followed by loading onto glass slides. Each slide was placed with 100 mg/ml of AO/EB staining solution and enclosed with coverslips. Finally, fluorescent microscope (Olympus, Japan) was used to assess morphology of α-mangostin-treated OVACAR-3 cells.

Assessment of mitochondrial membrane potential

To examine the mitochondrial membrane potential of OVCAR-3 cells, JC-1 staining assay was performed.

Briefly, OVACAR-3 cells were cultured onto 12-well plates for 12h followed by α-mangostin exposure for 24h with variant doses (0, 25, 100 and 200 μM). Afterwards, mitochondrial depolarization was estimated by using JC-1 mitochondrial membrane potential detection kit (Beyotime, China). RMPI-1640 culture medium was removed after α-mangostin treatment followed by washing of the cells with PBS. Treated OVACAR-3 cells were then placed in RMPI-1640 medium containing 10 mg/Ml JC-1 and incubated at 37°C for 30min. Prior to the estimation of mitochondrial membrane potential cells were washed thrice with PBS. Finally, fluorescent microscope (Olympus, Tokyo, Japan) was used to analyse two different forms of JC-1 i.e. aggregate and monomeric form.

Monitoring reactive oxygen species (ROS) production

To check the generation of intracellular ROS in α-mangostin treated OVACAR-3 cells, the ROS kit (Beyotime, China) was used. Briefly, OVACAR-3 cells were exposed to α-mangostin at varying doses (0, 25, 100 and 200 μM). Afterwards, treated OVACAR-3 cells were subjected to DCHF-DA (15mM) staining for half an hour at 37°C. Then, the cells were washed thrice with phosphate buffered saline (PBS) followed by suspending in PBS (500mL). Flow cytometer (ACEA NoVoCyte) was finally used to measure fluorescence.

Cell migration and invasion analysis

Transwell chambers migration and invasion assays were performed to analyze the cell migration and invasion potential of α-mangostin-treated human OVACAR-3 cells. Briefly, OVACAR-3 cells were transfected with variant α-mangostin doses (0, 25, 100 and 200 μM) for 24h. Afterwards, these transfected cells at a concentration of 1×10^5 cells were placed onto the upper transwell chambers containing RMPI-1640 medium, while the lower transwell chambers were placed only with 10% fetal bovine serum (FBS) (Corning Incorporated, Corning, NY, USA) and 600 μl RMPI-1640 medium. Thereafter, the chambers were incubated for 12h followed by fixation of cells with methanol for 10min at 4°C. Non-migrated cells were eliminated and 5min staining of migrated cells was accomplished with crystal violet at 25°C. Finally, a light microscope (TS100; Nikon Corporation, Tokyo, Japan) was used to analyze the migrated OVACAR-3 cells at 200x magnification. A similar procedure was performed for the determination of the invasion potential except coating of transwell chambers with Matrigel.

Western blotting analysis

The expressions of several cellular proteins in α-mangostin-treated human OVACAR-3 cells were examined through western blotting analysis. Briefly, OVACAR-3 cells were harvested at full growth confluence and subjected to α-mangostin exposure at variant doses (0, 25, 100 and 200 μM) for 24h. Afterwards, cells were lysed with RIPA lysis buffer and subjected to bicinchoninic acid (BCA) assay for quantification of protein content within each lysate. 40 μg of proteins from each lysate was placed onto SDS-PAGE followed by transference to nitrocellulose membranes, electrophoretically. Thereafter, TBST (tween) with TBS and non-fat dry milk (5%) were used to block these membranes at 4°C overnight. Afterwards, primary antibody treatment was instigated using antibodies against m-TOR, AKT, PI3K, Caspases (3, 8 and 9), Bax and Bcl-2. Primary treatment with antibodies was followed by secondary antibody exposure at room temperature for 2h. Finally, after washing twice with TBST, protein signals were observed through enhanced chemiluminescence assay kit (Thermo Scientific, United States).

Statistics

Difference between mean values were evaluated with Student's *t*-test, data was shown as mean±standard deviation and analyzed using SPSS software version 25.0. All the individual investigations performed in triplicate with $p<0.05$ as statistically significant.

Results

Cell proliferation inhibition by α-mangostin

To estimate the effects of α-mangostin molecule (Figure 1) on the cellular proliferation rate of OVACAR-3 cells, MTT assay was used. As uncontrolled proliferation is the dominating feature

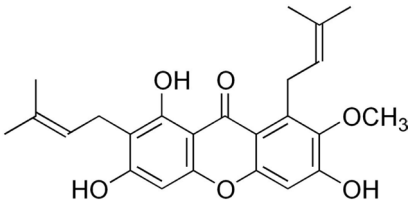

Figure 1. Chemical structure of α-mangostin molecule.

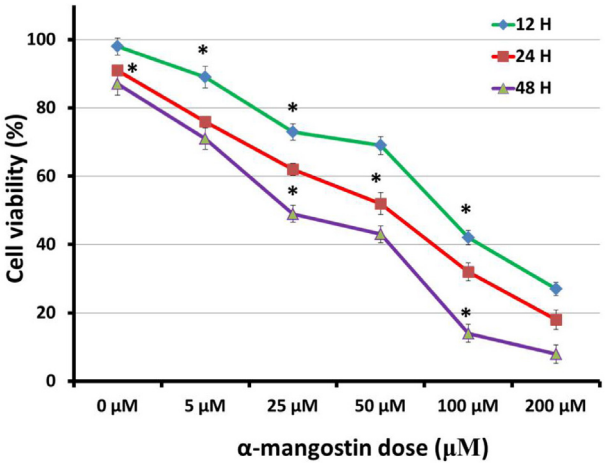

Figure 2. MTT assay results representing the viable cell percentage after α-mangostin treatment. OVACAR-3 cells were precultured for 24h followed by treatment with variant drug doses (0, 5, 25, 50, 100 and 200 μM) for indicated time intervals. Individual experiments were performed in triplicate and data are shown as mean±SD. *$p<0.05$ showed statistically significant difference.

of cancer cells, targeting it is one of the pivotal strategies in cancer research. OVACAR-3 cells were exposed to α-mangostin for different time intervals i.e. 12h, 24h and 48h and doses 0, 5, 25, 50, 100 and 200 μM. It was evident from the results that α-mangostin reduced the rate of proliferation in a time- and dose-dependent manner. After 12h of treatment the rate of proliferation reduced from almost 100% to 30% and after 24h of exposure the proliferation was limited to almost 20%, on higher drug doses. After extending the α-mangostin exposure for 48h, the proliferation was significantly supressed to almost 5% (Figure 2).

Suppression of clonogenic potential by α-mangostin in OVACAR-3 cells

The clonogenic potential of OVACAR-3 cells after α-mangostin exposure was testified by performing clonogenic assay. OVACAR-3 cells were exposed to variant α-mangostin doses for 12 days and afterwards colonies were numbered under a light microscope. The results indicated that the colonies of OVACAR-3 cells reduced remarkably with increasing α-mangostin doses (Figure 3A). The number of colonies in controls were observed as 350. After α-mangostin exposure the number of colonies reduced from 350 to almost 50 (Figure 3B).

α-mangostin induced morphological modifications in OVACAR-3 cells

Morphological modifications in OVACAR-3 cells were evaluated through phase contrast microscopy. The results indicated normal cell morphology in controls, while α-mangostin treated, OVACAR-3 cells showed significant changes in their morphology. These changes included membrane blebbing, plasma membrane rupture, cellular disintegration and nuclear condensation (Figure 4).

α-mangostin induced apoptotic cell death in OVACAR-3 cells

Apoptosis inducing potential of α-mangostin was examined through AO/EB staining assay. Apoptosis is a natural phenomenon of cell death under the circumstances of injury, stress, age and malfunctioning cells. Targeting apoptosis in a cancer cell has long served as a lead strategy to tackle cancer. AO/EB staining indicated that the number

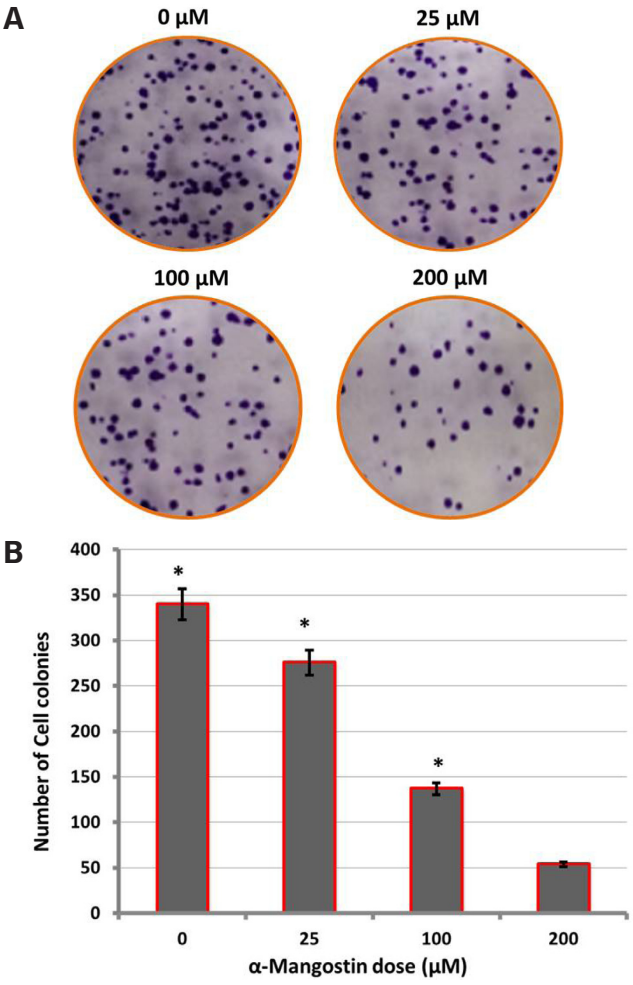

Figure 3. A: Figure representing the number of cell colonies in controls and after drug exposure at indicated doses via clonogenic assay. **B:** Graphical representation presenting the results of clonogenic assay after treatment of OVACAR-3 cells with α-mangostin. Individual experiments were performed in triplicate and data are shown as mean±SD. *p<0.05 showed statistically significant difference.

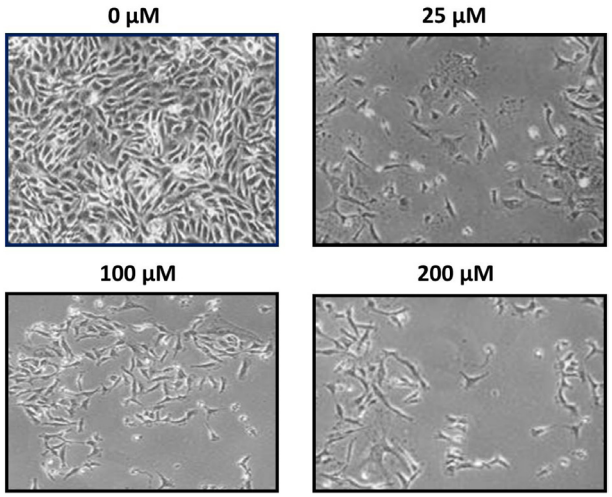

Figure 4. Pictures through phase contrast inverted microscope representing the morphology of OVACAR-3 cells after treatment with α-mangostin at designated doses. Cells in controls revealed normal cellular morphology in contrast to treated cells, which revealed membrane blebbing, plasma membrane rupture, nuclear condensation and cell disintegration. Individual experiments were performed in triplicate.

of apoptotic cells enhanced in comparison to controls in an α-mangostin dose-dependent manner (Figure 5). As evidenced from the results, early, late apoptotic and necrotic cells were observed in α-mangostin treated OVACAR-3 cells. Therefore, AO/EB staining assay indicated that the antiproliferative behaviour of α-mangostin against OVACAR-3 cells is mediated via apoptosis induction. Furthermore, western blotting assay revealed that the expression of anti-apoptotic protein Bcl-2 was significantly decreased in comparison to pro-apoptotic Bax protein, which enhanced with α-mangostin increased doses. The expression of Caspases (3, 8 and 9) were also observed to increase on α-mangostin treatment (Figure 6).

α-mangostin suppressed the mitochondrial membrane potential (MMP) and enhanced reactive oxygen species (ROS) in OVACAR-3 cells

JC-1 mitochondrial membrane potential detection kit was used to analyze the effect of α-mangostin on MMP in OVACAR-3 cells. MMP is an important parameter in apoptosis as reduced MMP results in the leakage of cytochrome c into the cytoplasm that initiates a cascade of reactions that ultimately result in apoptosis. The α-mangostin exposure of

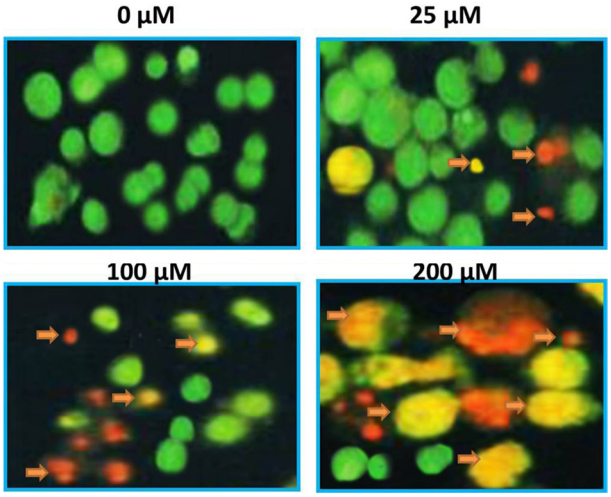

Figure 5. Results of AO/EB staining assay showing normal cells in controls and apoptotic cells in case of α-mangostin treatment. Arrows represent the early, late stage apoptotic and necrotic cells. Individual experiments were performed in triplicate.

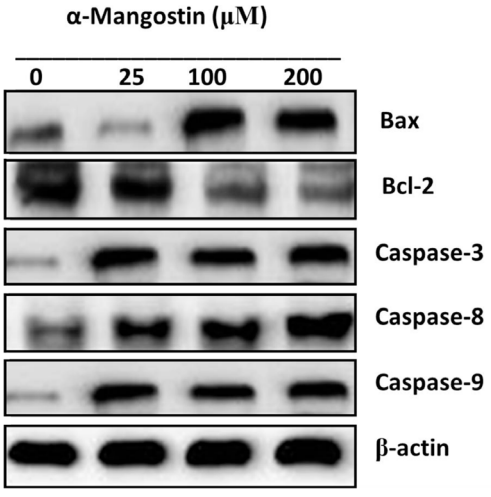

Figure 6. Western blotting assay presenting the levels of pro and anti-apoptotic proteins along with the levels of Caspases. The figure shows reduced activity of Bax and Bcl-2 and increased activity of Caspases (3, 8 and 9). Individual experiments were performed in triplicate.

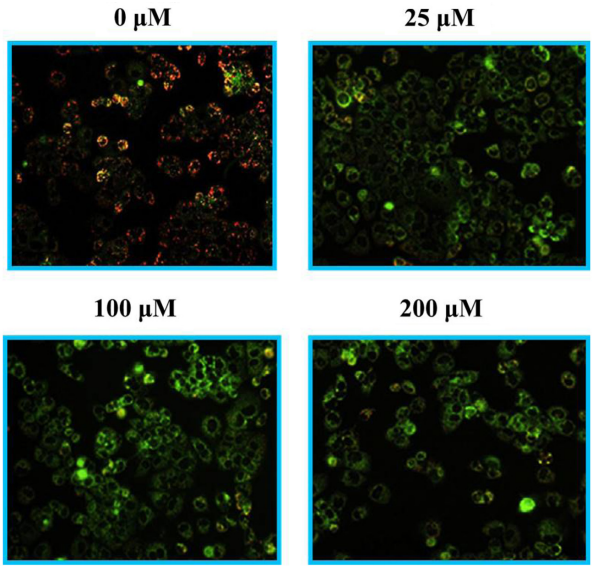

Figure 7. JC-1 staining assay results showing the reduced mitochondrial membrane potential (MMP) after α-mangostin treatment. Increased green fluorescence indicated reduced MMP. Individual experiments were performed thrice.

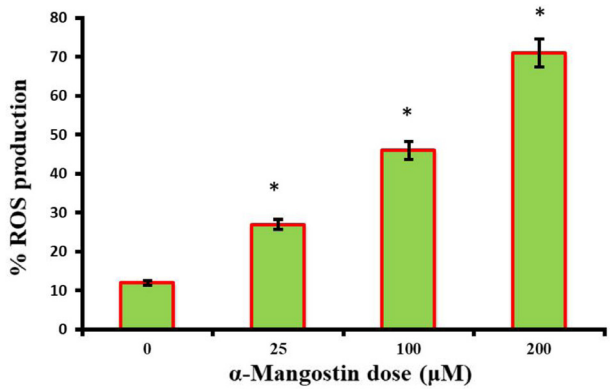

Figure 8. DCHF-DA staining assay presenting ROS in OVACAR-3 cells. Results showed enhanced ROS production in OVACAR-3 cells post α-mangostin treatment. Individual experiments were performed in triplicate and data are shown as mean±SD. *p<0.05 showed statistically significant difference.

OVACAR-3 cells reduced MMP significantly with a dose-dependent manner (Figure 7). Increased JC-1 fluorescence indicated decrease in MMP. The effect of α-mangostin on ROS production was evaluated through DCHF-DA staining assay. The results indicated potential rise in the intracellular ROS on α-mangostin treatment (Figure 8). Therefore, both MMP and ROS contributed to cytotoxicity of α-mangostin against human OVACAR-3 cells.

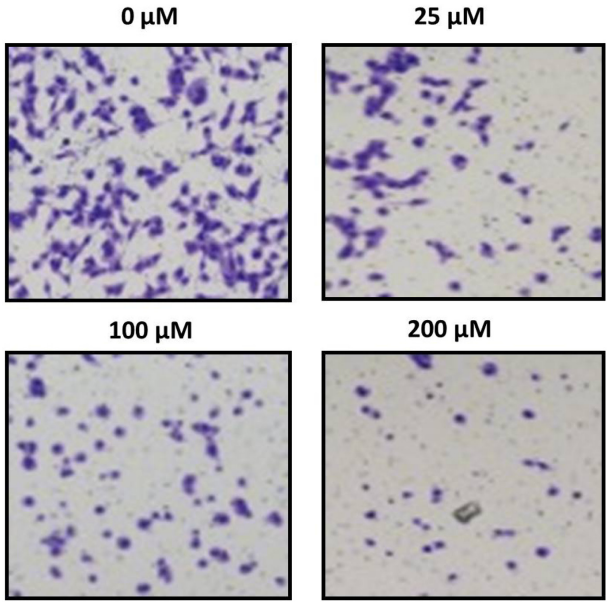

Figure 9. Transwell chambers assay results presenting the number of migrated OVACAR-3 cells after α-mangostin exposure. The figure demonstrates reduced number of migrated cells post α-mangostin treatment. Individual experiments were performed in triplicate.

α-mangostin inhibited the migration and invasion potential of OVACAR-3 cells

To analyse the cell migration and invasion of OVACAR-3 cells, transwell chambers assay was performed. Cell migration and invasion are the two important features of malignant metastatic cancer cell. Therefore, targeting cell migration and invasion is among the vital strategies to fight cancer metastasis. After treatment with varying α-mangostin doses (0-200 μM) OVACAR-3 cells were subjected to transwell chambers assay. The number of migrated cells were recorded to decline after α-mangostin treatment in comparison to controls (Figure 9). The effect of α-mangostin on invasion potential of OVACAR-3 cells showed that the number of invaded cells decreased dose-dependently (Figure 10). Therefore, α-mangostin reduced both cell migration as well as cell invasion potential of OVACAR-3 cells dose-dependently.

α-mangostin targeted m-TOR/PI3K/AKT signaling pathway in OVACAR-3 cells

The m-TOR/PI3K/AKT signaling pathway is among the vital pathways that regulate cell growth and differentiation. Western blotting assay was performed to assess the levels of m-TOR/PI3K/AKT signaling pathway related proteins in α-mangostin treated OVACAR-3 cells. The results showed that

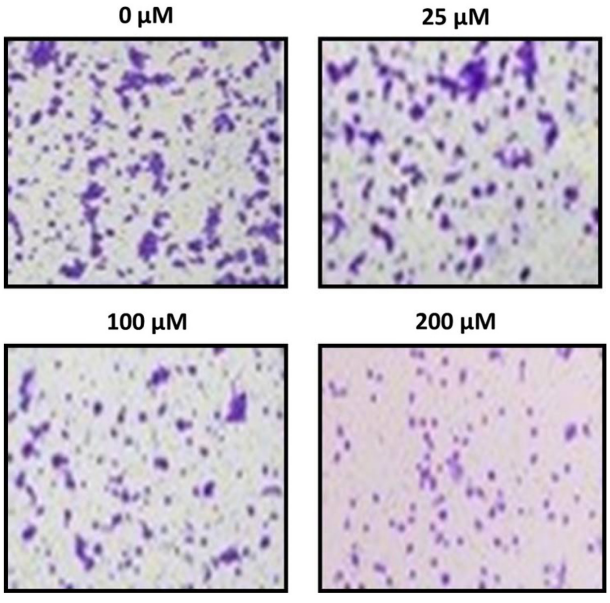

Figure 10. Transwell chambers assay results presenting the number of invaded OVACAR-3 cells after α-mangostin exposure. The figure demonstrates reduced number of invaded cells post α-mangostin treatment. Individual experiments were performed in triplicate.

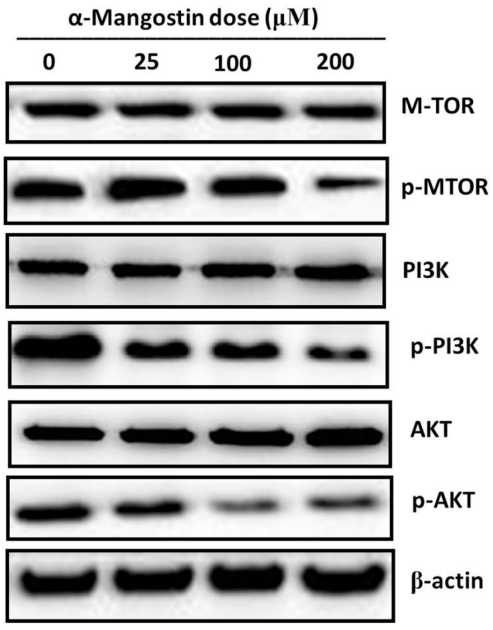

Figure 11. Western blotting assay presenting the levels of m-TOR/PI3K/AKT signaling pathway allied proteins in OVACAR-3 cells after α-mangostin exposure. Individual experiments were performed in triplicate.

the expressions of PI3K, AKT and m-TOR remained almost intact after α-mangostin exposure and those of phosphorylated PI3K, AKT and m-TOR reduced on increasing drug concentration (Figure 11).

Discussion

Ovarian cancer is a serious gynecological malignancy that needs to be addressed as soon as possible. There are several hurdles in ovarian cancer management, including distant metastasis, recurrence of disease, lack of efficient strategy and methodology, and even lethal side effects of current chemo-drugs. Therefore, novel therapeutic agents and targets are needed to tackle this malignancy. From the past three or four decades, apoptosis has been extensively targeted in cancer cells to achieve better results, as apoptosis is a normal process of programmed cell death that operates to maintain homeostasis of normal tissues and also eliminate damaged cells [17]. Apoptosis serves as a primary target of chemopreventives. Another strategy is to target pivotal signaling pathways that maintain cancer cell survival and differentiation. Lipid kinases (PI3K family) are regarded as key regulators of growth, differentiation and survival [18,19]. PI3K pathway bears numerous nodes that play important role in maintaining a large number of its functional outcomes [20]. The downstream targets of PI3K mediated via AKT includes mTOR (mammalian target of rapamycin), translation regulation in growth factor response by phosphorylation of the protein synthesis/manufacturing machinery and activation of cell proliferation [21]. Several studies have reported anticancer activity of α-mangostin mediated via targeting several cell signaling pathways. Herein, the current research was undertaken to investigate whether the anticancer effects of α-mangostin in OVACAR-3 human ovarian carcinoma cells are mediated via involvement of ROS, mitochondrial-mediated apoptosis, suppression of cell migration and invasion and m-TOR/PI3K/AKT signaling pathway which revealed that α-mangostin molecule possesses significant anticancer activity against ovarian cancer OVACAR-3 cells. MTT assay showed remarkable anti-proliferative potential of α-mangostin in a dose- and time-dependent manner. It inhibited clonogenic tendency of OVACAR-3 cells as well after 15 days of exposure. Furthermore, to demonstrate the underlying mechanism of the antiproliferative effects, apoptosis assessments were made which revealed that α-mangostin induces its cytotoxicity via apoptosis mediation and the apoptosis was itself regulated by caspase activation. Therefore, the apoptosis-inducing potential of α-mangostin was validated to be mitochondrial-mediated. Also, α-mangostin resulted in enhancement of ROS production in OVACAR-3 cells that ultimately resulted to cell death. Furthermore, cell migration and invasion potential of OVACAR-3 cells was suppressed by α-mangostin in a dose-dependent manner. Finally, the cell survival and differentiation regulatory pathway, that is m-TOR/PI3K/AKT signaling pathway, was significantly suppressed by α-mangostin exposure in OVACAR-3 cells.

Conclusion

The current investigation concluded that α-mangostin has a remarkable potential to inhibit proliferation of human ovarian cancer. The inhibition was found to be mediated via involvement of ROS, mitochondrial-mediated apoptosis, suppression of cell migration and invasion and reducing the m-TOR/PI3K/AKT signaling pathway. Therefore, α-mangostin can prove a lead molecule in ovarian cancer management.

Conflict of interests

The authors declare no conflict of interests.

References

1. Torre LA, Bray F, Siegel RL et al. Global cancer statistics, 2012. CA Cancer J Clin 2015;65:87-108.
2. Knutson KL, Karyampudi L, Lamichhane P, Preston C. Targeted immune therapy of ovarian cancer. Cancer Metastasis Rev 2015;34:53-74.
3. Au KK, Josahkian JA, Francis JA, Squire JA, Koti M. Current state of biomarkers in ovarian cancer prognosis. Fut Oncol 2015;11:3187-95.
4. Vaughan S, Coward JI, Bast RC et al. Rethinking ovarian cancer: recommendations for improving outcomes. Nat Rev Cancer 2011;11:719-25.
5. He QZ, Luo XZ, Wang K et al. Isolation and characterization of cancer stem cells from high-grade serous ovarian carcinomas. Cell Physiol Biochem 2014;33:173-84.
6. Newman DJ, Cragg GM. Natural products as sources of new drugs over the 30 years from 1981 to 2010. J Nat Prod 2012;75:311-35.

7. Graham JG, Quinn ML, Fabricant DS, Farnsworth NR. Plants used against cancer – an extension of the work of Jonathan Hartwell. J Ethnopharmacol 2000;73:347-77.
8. Yang G, Li X, Li X et al. Traditional chinese medicine in cancer care: a review of case series published in the chinese literature. Evid Based Complement Alternat Med 2012;2012:751046.
9. Jung HA, Su BN, Keller WJ, Mehta RG, Kinghorn AD. Antioxidant xanthones from the pericarp of Garcinia mangostana (Mangosteen). J Agric Food Chem 2006;54:2077-82.
10. Peres V, Nagem TJ, de Oliveira FF. Tetraoxygenated naturally occurring xanthones. Phytochemistry 2000;55:683-710.
11. Govindachari T, Kalyanaraman P, Muthukumaraswamy N, Pai B. Xanthones of (Garcinia mangostana Linn). Tetrahedron 1971;27:3919-26.
12. Dragendorff O. Uber das Harz von Garcinia Mangostana L. Justus Liebigs Annalen Chem 1930;482:280-301.
13. Matsumoto K, Akao Y, Kobayashi E et al. Induction of apoptosis by xanthones from mangosteen in human leukemia cell lines. J Nat Prod 2003;66:1124-7.
14. Sato A, Fujiwara H, Oku H, Ishiguro K, Ohizumi Y. ALPHA.-mangostin inducesCa2+-ATPase-dependent apoptosis via mitochondrial pathway in PC12 cells. J Pharmacol Sci 2004;95:33-40.
15. Matsumoto K, Akao Y, Ohguchi K et al. Xanthones induce cell-cycle arrest and apoptosis in human colon cancer DLD-1 cells. Bioorg Med Chem 2005;13:6064-9.
16. Shih YW, Chien ST, Chen PS, Lee JH, Wu SH, Yin LT. a-Mangostin suppresses phorbol 12-myristate 13-acetateinduced MMP-2/MMP-9 expressions via avb3 integrin/FAK/ERK and NF-jB signaling pathway in human lung adenocarcinoma A549 cells. Cell Biochem Biophys 2010;58:31-44.
17. Zucker RM, Hunter ES 3rd, Rogers JM. Confocal laser scanning microscopy of morphology and apoptosis in organogenesis-stage mouse embryos. Meth Mol Biol 2000;135:191-202.
18. Engelman JA. Targeting PI3K signalling in cancer: opportunities, challenges and limitations. Nat Rev Cancer 2009;9:550-62.
19. Vivanco I, Sawyers CL. The phosphatidylinositol 3-Kinase AKT pathway in human cancer. Nat Rev Cancer 2002;2:489-501.
20. Bader AG, Kang S, Zhao L et al. Oncogenic PI3K deregulates transcription and translation. Nat Rev Cancer 2005;5:921-9.
21. Wendel HG, De Stanchina E, Fridman JS et al. Survival signalling by Akt and eIF4E in oncogenesis and cancer therapy. Nature 2004;428:332-7.